

## STEADY-STATE SOLUTIONS IN NONLINEAR DIFFUSIVE SHOCK ACCELERATION

B. REVILLE AND J.G. KIRK

Max-Planck-Institut für Kernphysik, Heidelberg 69029, Germany

AND

P. DUFFY

UCD School of Physics, University College Dublin, Dublin 4, Ireland

*Draft version July 18, 2018*

### ABSTRACT

Stationary solutions to the equations of non-linear diffusive shock acceleration play a fundamental role in the theory of cosmic-ray acceleration. Their existence usually requires that a fraction of the accelerated particles be allowed to escape from the system. Because the scattering mean-free-path is thought to be an increasing function of energy, this condition is conventionally implemented as an upper cut-off in energy space — particles are then permitted to escape from any part of the system, once their energy exceeds this limit. However, because accelerated particles are responsible for substantial amplification of the ambient magnetic field in a region upstream of the shock front, we examine an alternative approach in which particles escape over a spatial boundary. We use a simple iterative scheme that constructs stationary numerical solutions to the coupled kinetic and hydrodynamic equations. For parameters appropriate for supernova remnants, we find stationary solutions with efficient acceleration when the escape boundary is placed at the point where growth and advection of strongly driven non-resonant waves are in balance. We also present the energy dependence of the distribution function close to the energy where it cuts off - a diagnostic that is in principle accessible to observation.

*Subject headings:* acceleration of particles — shock waves — methods: numerical — ISM: cosmic rays — ISM: supernova remnants

### 1. INTRODUCTION

It is widely thought that the diffusive acceleration of charged particles at shock fronts can be very efficient (for a review see Malkov & Drury 2001). The precise value of the efficiency is controlled by the microphysics of the injection of low-energy particles into the acceleration process, i.e., by processes operating on small length-scales. However, in the case of non-relativistic shocks, such as those encountered in supernova remnants, the bulk of the energy in nonthermal particles is carried off by those of the highest attainable energy, i.e., by particles that interact with relatively large length-scale structures.

Conventionally, the physics of this system is captured by combining a hydrodynamic description of the background plasma with the diffusion-advection equation obeyed by the distribution function of the accelerated particles. Analysis of the *stationary* solutions of these equations is the foundation on which the study of the overall efficiency of the process and the maximum energy to which particles can be accelerated rests.

The importance of stationary solutions was realized early on by Drury & Voelk (1981) who used a reduced, two-fluid description to analyze acceleration by plane shock fronts in a one-dimensional flow. Provided accelerated particles are not permitted to leave the system, the two-fluid description can be derived from the full description, including the diffusion-advection equation, using only two plausible assumptions about the particle distribution function. The more important of these is that the so-called *effective diffusion coefficient* is always positive. Drury & Voelk (1981) proved that this restricts the possible stationary flow patterns to those containing

a *precursor* in which the accelerated particles decelerate the incoming upstream flow, followed by a hydrodynamic shock front. This important result, which implies that only a finite number of stationary solutions exist for shocks of a given Mach number, was subsequently generalized to the relativistic case by Baring & Kirk (1991).

However, the relevance of these studies is questionable if the diffusion coefficient is an increasing function of particle energy, as is the case, for example, if the transport is dominated by scattering off Alfvén waves via the cyclotron resonance. One reason for this is that the timescale on which a stationary solution is approached becomes large at high particle energy. In this case, quasi-stationary solutions with a constant distribution function below a slowly evolving upper cut-off in energy can be expected to establish themselves, and have been found numerically by Bell (1987) and by Falle & Giddings (1987). Another reason is that, as particles are accelerated to higher and higher energy, their mean-free path increases, and at some point becomes comparable to the size of any realistic system. Thus, even if one considers only strictly stationary solutions, the escape of high-energy particles appears to be an important property that will limit the maximum energy to which particles can be accelerated in any given system.

One way of accounting for particle escape is to truncate the distribution function above some finite value of the energy. But even with this simplification, finding stationary solutions of the combined kinetic and hydrodynamic equations is much more difficult than solving the two-fluid system. An important advance was the discovery of an approximate analytic solution of the diffusion-advection equation by Malkov (1997a). This solution

has a particle distribution function that vanishes above an upper cut-off,  $p_{\max}$ , in the magnitude of the particle momentum. Wherever the hydrodynamic flow is compressed (usually throughout the precursor and at the shock front) there exists a flux of particles across this boundary in momentum space. These particles cease to contribute to the stress-energy tensor, and, therefore, effectively escape from the system. A similar distribution was adopted by Achterberg (1987) when investigating numerical solutions to this equation. Under this assumption it is possible to find approximate analytic solutions, and relatively straightforward to construct numerical solutions to the full set of equations (Achterberg 1987; Malkov et al. 2000; Blasi 2002; Amato & Blasi 2005).

Two problems intrinsic to this approach are immediately obvious. Firstly, the momentum dependence of the distribution close to  $p_{\max}$  — a diagnostic that is, in principle, accessible to observation — is not well-approximated. Secondly, the exclusion of a post-cursor, although made plausible by the two-fluid approach, is not always justified. The conditions that must be fulfilled by the distribution function and the momentum-dependent diffusion coefficient for this assumption to be valid (Kirk 1990) can in principle be checked *a posteriori*, but this is not straightforward for discontinuous distributions.

These problems arise because an upper cut-off in momentum is used to describe the physics of particle escape. Recently, however, observational evidence has been accumulating suggesting that cosmic rays are responsible for substantial amplification of the ambient magnetic field in the precursors of shock fronts in supernova remnants (Hwang et al. 2002; Vink & Laming 2003; Bamba et al. 2005; Uchiyama et al. 2007). This implies that the scattering mean-free-path is not only a function of energy, but also depends strongly on position with respect to the shock front. It, therefore, highlights a more serious short-coming of the approach that uses a cut-off in momentum space: The amplification of the field is likely to be connected with the spatial flux of energetic particles, which is artificially distorted if particles are assumed to vanish across a momentum boundary. In this paper we examine stationary solutions with escape through a spatial boundary instead of through a boundary in energy space.

Spatial boundaries have previously been implemented in Monte-Carlo simulations of the non-linear acceleration problem. In particular, Vladimirov et al. (2006) used a model equation to describe Alfvénic turbulence and coupled it to a Monte-Carlo simulation that permitted escape over a spatial boundary. In this way they were able to investigate the effects of an enhanced resonant interaction between the turbulent waves and the accelerated particles, although the position of the boundary itself remained arbitrary.

Recently, Zirakashvili & Ptuskin (2008) used MHD simulations to describe the excited turbulence and find the diffusion coefficient of the highest energy accelerated particles. They allowed these particles to escape over a spatial boundary, but used the test-particle approximation in which the flow speed is unaffected by the particles. In discussing shock fronts in supernova remnants, they suggested that the boundary leads the shock front by a distance given roughly by the radius of the remnant.

Our approach differs from these, not only in the nu-

merical method used to solve the acceleration problem, but also in the input physics. Resonant interactions between energetic particles and Alfvén waves were long thought to be responsible for coupling these particles to the background plasma (Bell 1978; MacKenzie & Voelk 1982; Achterberg 1983; Lucek & Bell 2000). However, well ahead of the shock front, non-resonant processes are more strongly driven and can be expected to dominate under the conditions present in supernova remnants (Bell 2004; Pelletier et al. 2006; Bykov & Toptygin 2005; Reville et al. 2007; Zirakashvili et al. 2008). In the linear phase, these instabilities inject short-wavelength turbulence into the plasma, resulting in a relatively large diffusion coefficient that is proportional to the square of the particle momentum (Zirakashvili & Ptuskin 2008). However, the non-linear evolution includes not only a cascade of energy to smaller length scales, but also the appearance of large-scale structures such as cavities (Bell 2005). In this regime, the mean-free-path is reduced, and its  $p^2$  dependence eliminated, as can be seen from large-scale numerical simulations of the transport properties (Reville et al. 2008). These simulations have not yet advanced to the stage where they can provide a model diffusion coefficient over a wide dynamic range of momentum. Consequently, we model this effect by assuming the diffusion to be of Bohm type in a background field that is amplified to the value at which the non-resonant instabilities are expected to saturate. Although this is a relatively crude approach, it enables us to solve the non-linear problem of finding stationary solutions. We are then able to check the location of the spatial boundary, which should be located where the growth rate of the non-resonant modes is approximately equal to the speed of advance of the shock divided by the distance from the shock front. Since the escaping flux is dominated by the highest energy particles, we do not expect that changing the form of the diffusion coefficient will alter significantly our conclusions, provided it remains an increasing function of momentum.

The paper is set out as follows: In Section 2 we set up the advection-diffusion equation and the hydrodynamic equations governing the system of accelerated particles and background plasma. The two ways of allowing for particle escape are discussed in Section 3. In Section 4 we describe the iteration and finite difference methods used to find stationary solutions of the combined advection-diffusion and hydrodynamic equations using the two different boundary conditions, and in Section 5 we compare and discuss the results. A discussion of the self-consistency of the position of the spatial boundary and a summary of our conclusions is presented in Section 6.

## 2. BASIC EQUATIONS

We consider a gas subshock located at  $x = 0$  with a flow profile, in the subshock rest frame, given by

$$U(x) = \begin{cases} u_2 & x > 0 \\ u(x) & x \leq 0 \end{cases}$$

with  $u(x = 0^-) = u_1$  and  $u_2$  constant in the absence of a post-cursor. The gas velocity far upstream is denoted by  $u_0$ . We assume that, as a result of scattering centres frozen into the flow, energetic particles, with speeds  $v \gg u(x)$ , undergo diffusion with a momentum-dependent diffusion coefficient  $\kappa(p)$ . These particles are

also advected with the flow, adiabatically compressed and injected from the thermal background. The isotropic part of their phase space density obeys the transport equation (Skilling 1975)

$$\frac{\partial f}{\partial t} + U \frac{\partial f}{\partial x} - \frac{\partial}{\partial x} \left( \kappa \frac{\partial f}{\partial x} \right) = \frac{1}{3} \frac{dU}{dx} p \frac{\partial f}{\partial p} + Q_0(x, p), \quad (1)$$

where  $Q_0$  describes the injection of particles into the acceleration process. For mono-energetic injection at the gas subshock

$$Q_0(x, p) = \frac{\eta n_{g,1} u_1}{4\pi p_0^2} \delta(p - p_0) \delta(x),$$

where the number density of gas particles entering the shock front is  $n_{g,1}$  and  $\eta$  is the fraction of entering particles that take part in the acceleration process. In our notation, the particle mass and momentum are  $m$  and  $mcp$ , so that  $p$ ,  $p_0$  etc. are dimensionless, and the phase-space distribution function  $f$  has the dimensions of an inverse volume.

Integrating Eq. (1) first across the shock and then across the injection momentum, it follows that

$$f_0(p_0) = \frac{3u_1}{\Delta u} \frac{\eta n_{g,1}}{4\pi p_0^3} \quad (2)$$

with  $\Delta u = u_1 - u_2$ . An important restriction on this approach is that the distribution function at the injection momentum  $p_0$  must be approximately isotropic. This requires that the velocity of these particles should be several times greater than that of the upstream plasma. Since we will be interested primarily in shocks in supernova remnants, where  $u_0/c \lesssim 1/30$  we require  $p_0 \geq 0.1$ .

In this paper we are interested in steady state solutions to the particle transport equation, and in particular the role played by particle escape, when the pressure associated with the energetic particles

$$P_{\text{cr}}(x) = \frac{4\pi}{3} mc^2 \int_{p_0}^{\infty} v p^3 f(x, p) dp \quad (3)$$

reacts on the flow. Sufficiently far upstream, in the absence of cosmic rays, the gas has a density  $\rho_0$  and pressure  $P_{g,0}$ . Mass and momentum conservation give

$$\rho(x)u(x) = \rho_0 u_0, \quad (4)$$

$$P_{\text{cr}}(x) + \rho(x)u(x)^2 + P_{g,0} \left( \frac{u(x)}{u_0} \right)^{-\gamma} = \rho_0 u_0^2 + P_{g,0} \quad (5)$$

where  $\gamma$  is the adiabatic index of the gas.

The plasma flowing towards the shock is adiabatically compressed and slowed in the precursor. Its velocity profile  $u(x)$  is a monotonic function. Non-adiabatic heating is potentially important (e.g. Caprioli et al. 2008; Vladimirov et al. 2008). However, in the interests of simplicity, we shall neglect it in the following. For adiabatic heating alone, the sub-shock compression ratio  $r_s = u_1/u_2$  and the pre-compression

$$R = u_0/u_1. \quad (6)$$

are related by (see, for example Landau & Lifshitz 1959)

$$r_s = \frac{\gamma + 1}{\gamma - 1 + 2R^{\gamma+1}M^{-2}}, \quad (7)$$

where  $M$  is the Mach number of the flow at upstream infinity. For a given pre-compression ratio, we can use

Bernoulli's equation (5) to determine the cosmic-ray pressure at the shock

$$\frac{P_{\text{cr}}(0^-)}{\rho_0 u_0^2} = 1 - R^{-1} + \frac{1}{\gamma M^2} (1 - R^\gamma). \quad (8)$$

Thus, given the upstream conditions and  $R$ , or, alternatively,  $r_s$ , we can determine the cosmic-ray pressure at the shock.

### 3. PARTICLE ESCAPE

#### 3.1. Boundary in energy

As mentioned in Section 1, most previous analytic and semi-analytic calculations adopted a precursor of infinite spatial extent. Escape is permitted by assuming that particles with energy above a certain threshold decouple from the plasma. In essence, this is equivalent to assuming that the mean-free-path to scattering is energy dependent, and, above a certain threshold, becomes large compared to the size of the system. In the resonant scattering scenario, this implies that the relevant wave spectrum cuts-off above a certain wavelength.

Since the most energetic particles are highly relativistic an upper cut-off in the energy is equivalent to one in the magnitude of the momentum. For  $p > p_{\text{max}}$ , particles escape from the system, and the approximate steady-state solution for  $p < p_{\text{max}}$  is

$$f(x, p) = f_0(p) \exp \left[ \frac{q}{3\kappa} \left( 1 - \frac{u_1}{u_2} \right) \int_x^0 dx' u(x') \right], \quad (9)$$

where  $q = \partial \ln f_0 / \partial \ln p$ . The additional factor of  $(1 - u_2/u_1)$  was included in Blasi et al. (2007) to match the boundary condition for weakly modified shocks. The distribution at the shock, for monoenergetic injection, is

$$f_0(p) = \frac{3Rr_s}{Rr_s U(p) - 1} \frac{\eta n_0}{4\pi p_0^3} \exp \left[ - \int_{p_0}^p \frac{dp'}{p'} \frac{3Rr_s U(p')}{Rr_s U(p') - 1} \right] \quad (10)$$

where  $U(p) = u_p(p)/u_0$  with

$$u_p(p) = u_1 - \frac{1}{f_0} \int_{-\infty}^{0^-} dx \frac{du}{dx} f(x, p). \quad (11)$$

Following Blasi (2002) we take  $U(p_0) \approx R^{-1}$  to give

$$\eta = 4\pi p_0^3 f_0(p_0) \frac{r_s - 1}{3n_0 R r_s} \quad (12)$$

in agreement with equation (2). In the results of this work, we will adopt the dimensionless injection parameter,  $\nu$ , as defined in Malkov et al. (2000),

$$\nu = \frac{4\pi}{3} \frac{mc^2}{\rho_0 u_0^2} p_0^4 f_0(p_0), \quad (13)$$

where again,  $p$  is dimensionless.

#### 3.2. Boundary in space

A free-escape boundary upstream implies that all particles that cross a surface placed at a distance  $L_{\text{esc}}$  upstream of the shock leave the system. Essentially, the particle mean-free-path and, therefore, the diffusion coefficient, become infinite at the escape boundary due to the absence of scattering waves beyond that point. Since we employ a diffusion approximation, this can be implemented by setting the isotropic part of the distribution to

zero on the boundary. Whilst inside, we assume particles undergo Bohm diffusion,

$$\kappa = \kappa_0 p, \quad x > -L_{\text{esc}} \quad (14)$$

Higher energy particles have a larger mean-free-path and, therefore, propagate from the shock to the boundary more easily than low energy ones. Since they then escape, a turn-down in the spectrum results. However, this is a smooth decrease, rather than an abrupt cut-off. It occurs close to a momentum  $p^*$  defined by

$$L_{\text{esc}} = \kappa(p^*)/u_0, \quad (15)$$

In the test particle limit, where the upstream flow is unmodified and constant, a straightforward calculation shows that the spectrum at the shock,  $f_0(p)$ , has a slope given by

$$-\frac{d \ln f_0}{d \ln p} = \frac{3u_1}{\Delta u} \frac{1}{[1 - \exp(-L_{\text{esc}}u_0/\kappa)]} \quad (16)$$

At low momenta,  $p \ll p^*$ , the spectrum agrees with the standard test-particle result without escape upstream, but at high momenta  $p \sim p^*$  the spectrum cuts off exponentially. It should be noted that some particles with momenta  $p \leq p^*$  also reach the escape boundary, and the spectrum will start to turn over at these values. Although the particle distribution function  $f$  vanishes at the free-escape boundary, the particle flux remains finite, being proportional to  $p^2 \kappa \partial f / \partial x$ . In the test-particle approximation it can be written, making the substitution  $s = p/p^*$ ,

$$-s^2 \kappa \frac{\partial f}{\partial x} = \frac{u_0 f_0(p_0) s^2}{e^{1/s} - 1} \exp \left[ \frac{-3r_s}{r_s - 1} \int_{s_0}^s \frac{d \ln s'}{1 - e^{-1/s'}} \right] \quad (17)$$

where  $s_0 = p_0/p^*$ . As a function of momentum, the escaping flux is sharply peaked at  $s \approx (r_s - 1)/(r_s + 2)$ .

#### 4. METHOD OF SOLUTION

In the case of a boundary in energy, we use an iteration scheme similar to that employed by Amato & Blasi (2005). Given a shock Mach number  $M$ , shock speed  $u_0$  and momentum range  $p_0, p_{\text{max}}$ , we look for converged solutions for each value of  $R$ . The initial flow profile is linear, and the spectrum is a single power law. This allows us to calculate  $U(p)$  from which we determine the injection parameter  $\eta$  in Eq (10), by identifying the cosmic ray pressure at the shock front in Eq (5) with the integral over  $p$  of  $vp^3 f_0$ , as indicated by Eq (3). Using equations (9) and (3) we then update the flow using the fluid equations. This gives new values for  $u(x)$  and  $q(p)$ , and, hence a new value for  $\eta$ . This is repeated until  $\eta$  has converged.

Numerical solutions for steady state modified shocks and particle spectra, with a free escape boundary upstream, are also found using an iterative procedure. For a given Mach number ( $M$ ), shock speed ( $u_0$ ) and pre-compression ratio ( $R$ ), we initialize the spectrum using the test particle solution. The flow profile is then adjusted using the flux conservation equations (4,5). With the modified flow, the distribution function is updated by solving the time dependent transport equation for particles, equation (1), with the upstream boundary condition  $f(-L_{\text{esc}}, p) = 0$ . For this we use a Crank-Nicholson scheme centred in space and upwind in momentum. Using Eq. (8), the distribution function can be normalized

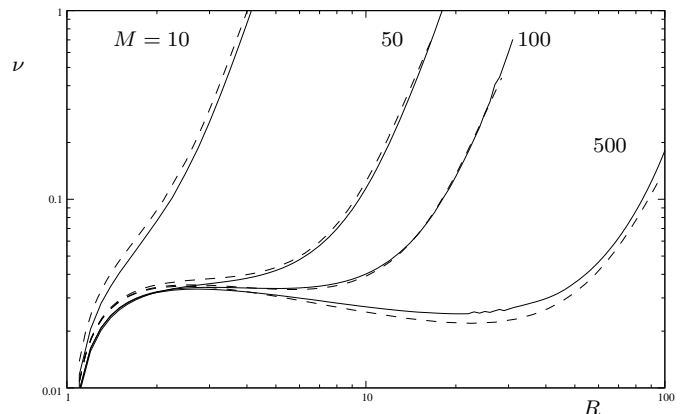


FIG. 1.— The injection parameter  $\nu$  as a function of the pre-compression  $R$  — see Eq. (6) — for increasing Mach number at a fixed upstream velocity  $u_0 = 5,000 \text{ km s}^{-1}$ . In generating this plot, we set  $p_0 = 0.1mc$  and  $p^* = p_{\text{max}} = 10^3 mc$ . The solid lines are found using a spatial boundary, the dashed lines use a boundary in energy.

to match the pressure at the shock. When, at each iterative step, the transport equation is solved, the resulting cosmic ray pressure is used to update the flow which, in turn, is then used to update the particle distribution.

The solution is found when the fluid quantities no longer change and the injection parameter  $\eta$  has converged. The code steps through values of the pre-compression ratios, using the previous converged profile and spectrum as the initial conditions for the next iteration. In this manner we obtain a full set of solutions that depend on  $\eta, M, R$  and  $L_{\text{esc}}$ .

## 5. RESULTS

### 5.1. Comparison of approaches

In order to make a meaningful comparison between the two methods we take

$$p^* = p_{\text{max}} \quad (18)$$

so that the boundary for upstream spatial escape, characterized by  $L_{\text{esc}}$ , is placed one diffusion length away from the shock for particles with momentum  $p_{\text{max}}$ . Consequently, the gradual momentum cut-off produced by the spatial boundary technique is close to the position of the abrupt momentum boundary.

Figure 1 plots the numerically determined injection parameter  $\nu$  as a function of the pre-compression ratio for the two different methods. These plots follow a similar form to those studied analytically by Malkov (1997b). The curve for each shock Mach number can, in general, be separated into three different regimes. The inefficient weakly modified regime where the spectrum resembles the test particle solution, the efficient regime where the shock is strongly modified, with a weak subshock, and an intermediate regime between the two. This intermediate regime lies typically in a narrow range of the injection parameter  $\nu$ . As the shock Mach number increases, multiple solutions for a single value of  $\nu$  occur, as found by Malkov (1997b); Amato et al. (2008). The two approaches give similar results, as expected, since the normalization of the spectrum is fixed by Eq (8). The differences arise due to the shape of the spectrum close to the cut-off. In Fig 2 we show the  $\nu - R$  diagram

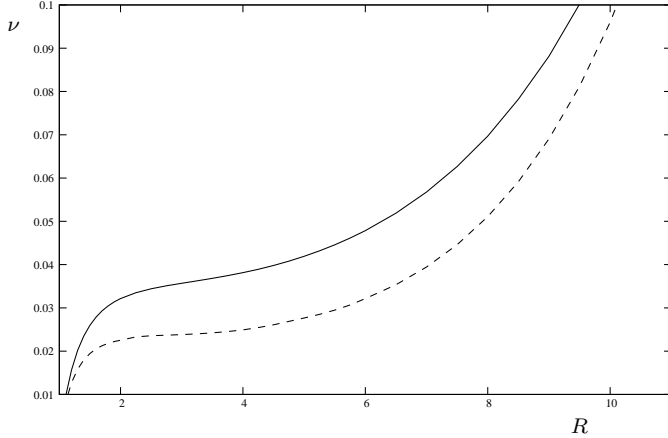


FIG. 2.— The injection parameter  $\nu$  as a function of the pre-compression ratio  $R$  for a  $M = 50$  shock using different injection and escape momenta. Solid:  $p_0 = 0.1mc$ ,  $p^* = 10^3mc$ , dashed:  $p_0 = 0.1mc$ ,  $p^* = 10^4mc$ .

for a Mach 50 shock for different values of maximum and minimum momentum using the free-escape boundary.

Figures 3 and 4 compare the flow and pressure profiles, as well as the spectrum and spectral index for Mach numbers,  $M = 100$  and  $M = 500$ . Both examples are with a pre-compression ratio of  $R = 20$ . As can be seen from Fig. 1, the two cases fall in different regimes. For the  $M = 100$  case, the shock is strongly modified with  $r_s \approx 2.1$ , while the  $M = 500$  case is in the intermediate regime with a subshock compression ratio of  $r_s \approx 3.86$ . This can be seen from the low energy shape of the spectrum: the reduced sub-shock compression leads to a much softer spectrum at the  $M = 100$  shock.

The flow profiles of the two models differ only slightly. This follows naturally from the boundary conditions: with a free escape boundary, the precursor length is fixed by  $L_{\text{esc}}$ . Using a boundary in momentum leads to a slightly extended precursor, due to the larger number of particles with momenta  $p^*$  interacting on a slightly larger scale. For both Mach numbers, there is a smooth turnover in the spectrum at momenta close to  $p^*$ . Furthermore, the momentum derivative of the distribution remains negative in this range. In this case, it can be shown (Kirk 1990, Eq (12)) that the dynamics of particles close to  $p^*$  do not permit a post-cursor. However, the possibility remains that the dynamics of the injection mechanism may still do so (Zank et al. 1993). Particles with momenta slightly less than  $p^*$  are also able to diffuse a distance  $L_{\text{esc}}$  from the shock and escape upstream. This is what leads to the observed turn-over. The reduced value for  $p^*$  is due to the non-linear effects of the system, and a crude estimate of the reduction is given by the formula

$$p_{\text{eff}}^* = \frac{p^*}{u_0 L} \int_L^{0^-} u dx. \quad (19)$$

### 5.2. Location of the spatial boundary

In our approach, we assume turbulence is generated at the spatial boundary by a non-resonant instability driven by particles escaping into the undisturbed upstream medium. The condition that these waves are strongly driven is

$$\zeta M_A^2 \geq 1, \quad (20)$$

(Bell 2004) where

$$\zeta = \frac{j_{\text{cr}} p_{\text{eff}}^* mc}{e \rho_0 u_0^2} \quad (21)$$

and  $M_A$  is the Alfvén Mach number of the shock, in the medium upstream of the boundary.

The cosmic-ray current is evaluated from integration of the diffusive flux over momentum space

$$j_{\text{cr}}(x) = -4\pi e \int_{p_0}^{\infty} \kappa \frac{\partial f}{\partial x} p^2 dp. \quad (22)$$

The integrand in this function peaks close to  $p = p^*$  and can be easily extracted from the numerical solution to the full non-linear problem. Because the magnetic field ahead of the boundary is not specified in the solutions, we plot  $\zeta M^2$  rather than  $\zeta M_A^2$  as a function of the precursor compression  $R$  in Fig. 5. In the medium surrounding a supernova remnant, we expect  $M_A \sim M$ . Therefore, according to this figure, the non-resonant waves are indeed strongly driven, as defined by Eq. (20). In agreement with the linear theory, we find that  $j_{\text{cr}}(-L)$  is an increasing function of the shock's Mach number and a decreasing function of  $p^*$ . For fixed maximum momentum, this result is independent of the diffusion coefficient in the precursor, and, therefore, of the strength of the amplified magnetic field — a weaker field leads to a larger precursor but does not change the escaping particle flux.

The assumption that particles escape freely upstream of the boundary implicitly assumes that the instability responsible for the generation of the turbulence operates on a length scale that is short compared to the precursor length. This requires that the inverse of the maximum growth rate  $\gamma_{\text{max}}$  of the non-resonant instability should be less than the advection time through the precursor. The maximum growth rate is related to the driving parameter by

$$\gamma_{\text{max}} = \frac{\zeta M_A u_0}{2r_g(p_{\text{eff}}^*)} \quad (23)$$

where the gyro-radius of escaping particles is evaluated in the ambient magnetic field  $B_0$  upstream of the boundary. It is convenient to define the advection length

$$L_{\text{adv}} = \frac{u_0}{\gamma_{\text{max}}}. \quad (24)$$

However, the length scale in our numerical simulation is set by the value of the diffusion coefficient in the amplified magnetic field  $B_s$ . Relating this to the diffusion coefficient by assuming Bohm diffusion gives the following lengthscale for our hydrodynamic precursor:

$$L_{\text{pc}} = \frac{cr_g(p^*)}{3u_0} \left( \frac{B_0}{B_s} \right). \quad (25)$$

The ratio of these two length scales is an important parameter

$$\frac{L_{\text{adv}}}{L_{\text{pc}}} = \frac{6}{\zeta} \frac{v_A}{c} \left( \frac{B_s}{B_0} \right) \left( \frac{p_{\text{eff}}^*}{p^*} \right). \quad (26)$$

and, in order to evaluate it, we must estimate the strength of the amplified field. Bell (2004) and Pelletier et al. (2006) give the following approximation for the saturated magnetic field energy density:

$$\frac{B_s^2}{8\pi} \approx \frac{3u_1}{2c} P_{\text{CR}}(0^-). \quad (27)$$

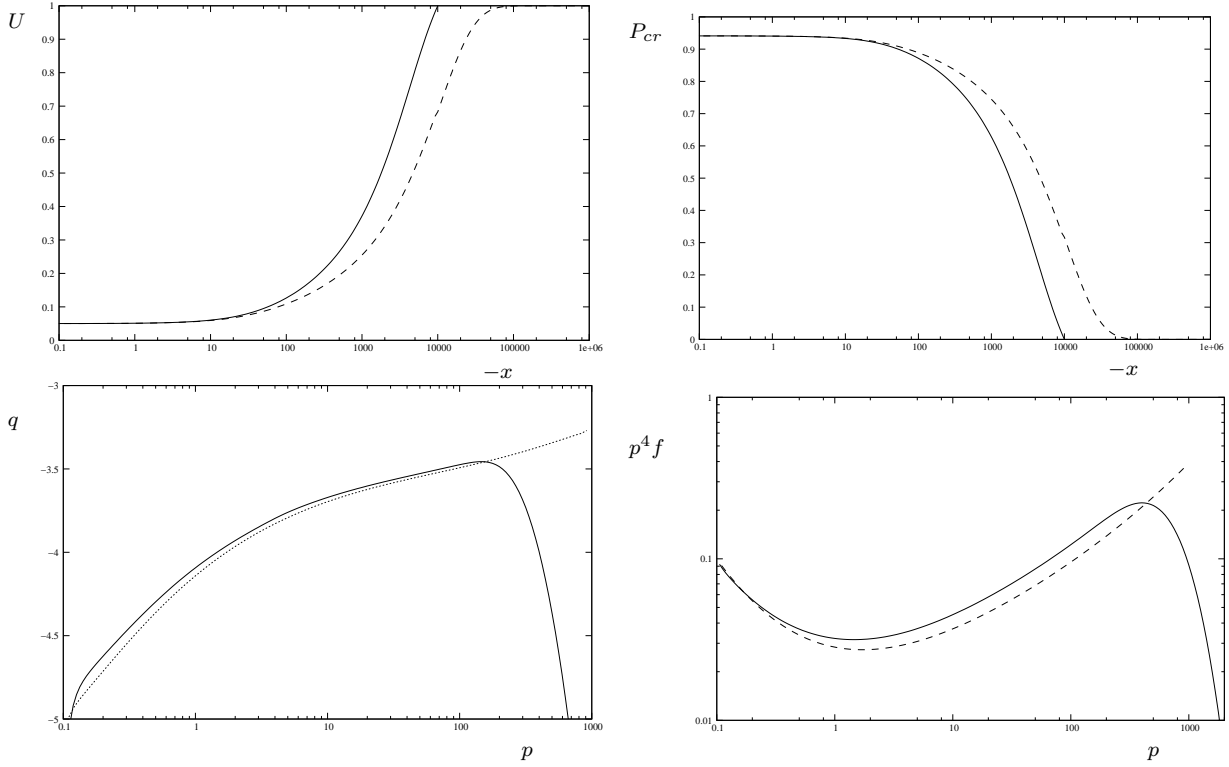


FIG. 3.— Normalized cosmic-ray pressure and flow profile for a  $M = 100$  shock, as a function of distance upstream of the sub shock. The pre-cursor compression ratio is  $R = 20$ . The solid lines correspond to the spatial boundary approach and dashed lines to the momentum boundary.

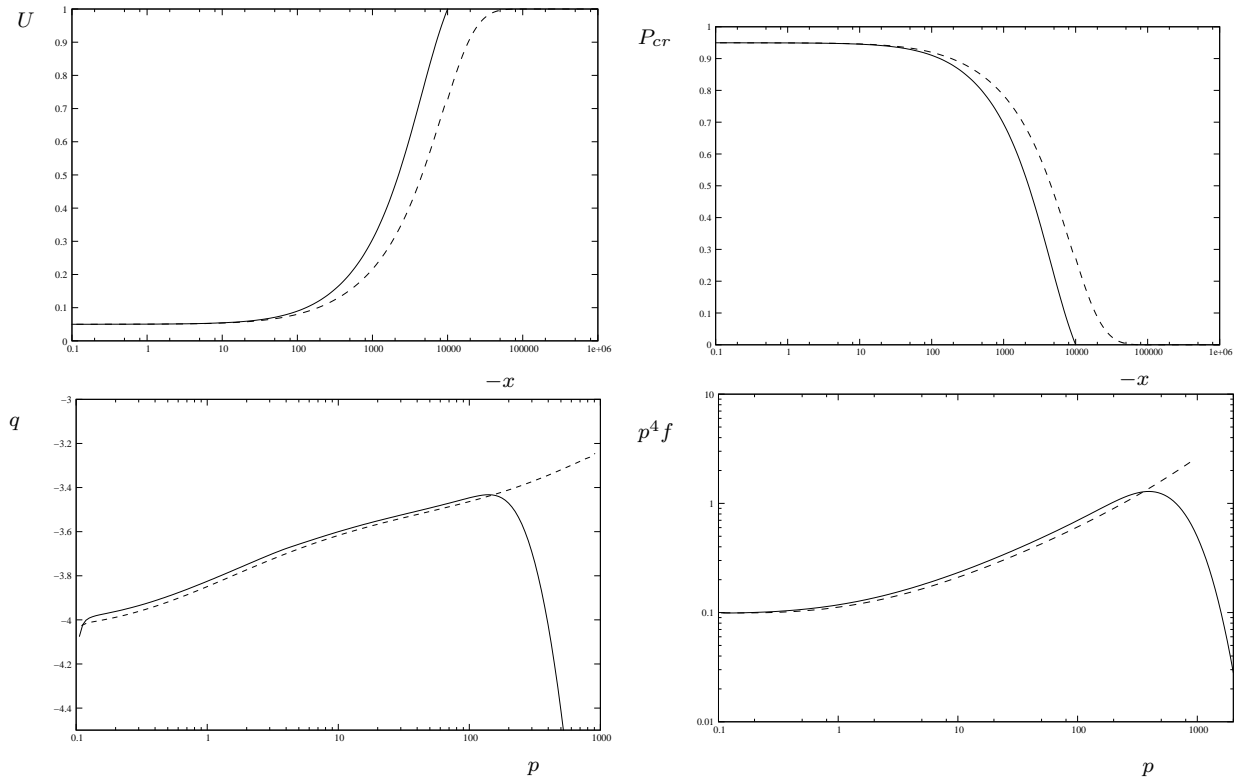


FIG. 4.— Normalized cosmic-ray pressure and flow profile for a  $M = 500$  shock, as a function of distance upstream of the sub shock. The pre-cursor compression ratio is  $R = 20$ . The solid lines correspond to the spatial boundary approach and dashed lines to the momentum boundary.

Numerical investigations of the non-linear behavior of magnetic turbulence in the presence of streaming cosmic rays have been performed (e.g. Niemiec et al. 2008; Riquelme & Spitkovsky 2008), but the results concerning the saturation level of this instability are inconclusive. Adopting Eq.(27), and substituting into Eq.(26) we find

$$\frac{L_{\text{adv}}}{L_{\text{pc}}} = \frac{6\sqrt{3}}{\zeta} \left(\frac{u_0}{c}\right)^{3/2} \left(\frac{P_{\text{CR}}(0^-)}{R\rho_0 u_0^2}\right)^{1/2} \left(\frac{p^*_{\text{eff}}}{p^*}\right). \quad (28)$$

We plot  $L_{\text{adv}}/L_{\text{pc}}$  determined numerically according to Eq.(28) as a function of the injection parameter  $\nu$  in Fig. 6, for  $M = 100$ . For weakly modified shocks with  $r_s \approx 4$ , the non-resonant instability grows slowly ahead of the escape boundary:  $L_{\text{adv}} \gg L_{\text{pc}}$ . For intermediate strength modified shocks  $4 \lesssim R \lesssim 10$  (see Fig. 1 to relate  $\nu$  to  $R$ ), the growth time is comparable to the advection time. For highly modified shocks,  $R > 10$ , the instability grows very rapidly in a small region just ahead of the escape boundary.

Formally, the calculations we present are valid only in this latter case, where the region in which the magnetic field increases from its ambient strength to its strength in the precursor is small compared to the length of the precursor itself. However, the point at which amplification sets in is arbitrary in this case. The flux of particles escaping from the shock front remains constant in planar geometry, so that we should expect the pre-cursor length to increase as these particles penetrate further and further upstream. This leads to a higher  $p^*$  and reduces the flux of escaping particles. In a fully self-consistent picture, this process should regulate itself such that the advection length becomes comparable to the precursor length.

On the other hand, for weakly modified shocks, where  $L_{\text{adv}} \gg L_{\text{pc}}$ , the escaping particles must penetrate a large distance in front of the shock before the instability they drive has time to grow appreciably. In essence, this is the situation investigated by Zirakashvili & Ptuskin (2008), who assumed the precursor to the shock — which is the region where the hydrodynamics are influenced by the accelerated particles — was very short compared to the other length scales in the problem. According to our results, this situation is consistent with stationarity of the accelerated particle spectrum only for weakly modified shocks that are relatively inefficient. In this case, however, the magnetic field is amplified very gradually, and the approximation that the amplification region is short compared to the pre-cursor is inconsistent. This is because a level of turbulence close to that assumed in the precursor is already available and able to interact with particles far ahead of the escape boundary. This again suggests that, in a self-consistent picture, the precursor length will be comparable to the advection length of the instability.

According to Fig. 6, the value of  $\nu$  at which the ratio of  $L_{\text{adv}}$  to  $L_{\text{pc}}$  is unity is a decreasing monotonic function of  $p^*$ , suggesting the physical picture evolves in the following manner: For a given injection parameter  $\nu$  and momentum  $p^*$ , determined from the length of the precursor, we can calculate the ratio of the advection length to the precursor length. If this ratio is large the escape boundary is too far from the shock and  $p^*$  will reduce itself until the ratio reaches unity. If, however, the ratio is too

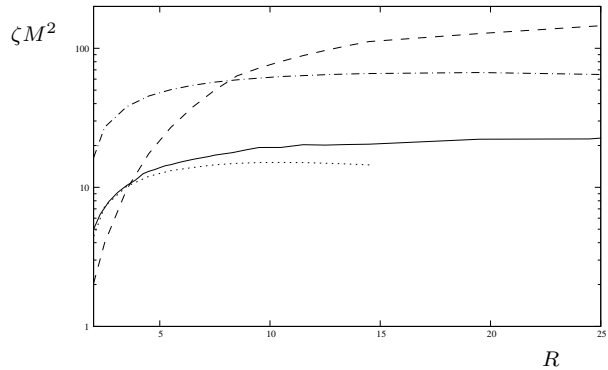


FIG. 5.— The driving parameter  $\zeta$  times the square of the sonic Mach number  $M$  as a function of subshock compression for different parameters. Over the entire parameter range  $\zeta M^2 \gg 1$ . Therefore, provided the plasma  $\beta \equiv M^2/M_A^2$  is not too large, the non-resonant mode is, according to Eq. (20), the fastest growing mode. The lines correspond to  $M = 500$ ,  $p^* = 10^4$  (dashed),  $M = 100$ ,  $p^* = 10^5$  (solid),  $M = 100$ ,  $p^* = 10^4$  (dash-dot),  $M = 50$ ,  $p^* = 10^4$  (dotted), with an injection momentum of  $p_0 = 0.1$ .

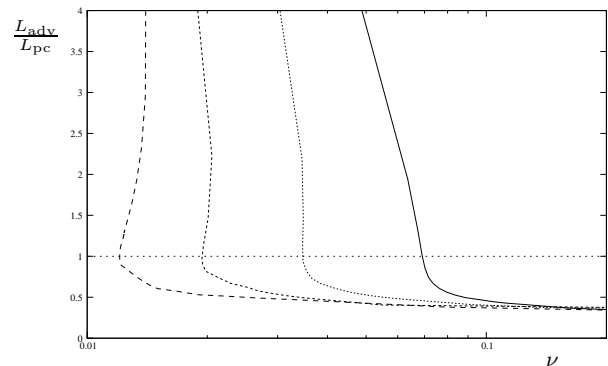


FIG. 6.— The ratio of advection length to precursor length,  $L_{\text{adv}}/L_{\text{pc}}$ , for different values of  $p^*$  for a shock Mach number of 100. From left to right the lines correspond to  $p^* = 10^5$ ,  $p^* = 10^4$ ,  $p^* = 10^3$ ,  $p^* = 10^2$ . All models were calculated using an injection momentum of  $p_0 = 0.1$ . The horizontal line corresponds to  $L_{\text{adv}} = L_{\text{pc}}$ .

small,  $p^*$  will increase, as described above. In general, in the range of precursor compression ratios that interest us here,  $\nu$  is a decreasing function of  $p^*$  (Malkov & Drury 2001), which can be clearly seen in Fig. 2. It is natural to expect that the system will organize itself such that the advection length approaches the precursor length. For the parameters adopted in Fig. 6, this occurs for shocks in the intermediate range of modification.

This scenario suggests there exists a relationship between the injection and the maximum momentum in the system. A similar connection has previously been investigated by Malkov et al. (2000) in the context of self-organized criticality in cosmic-ray modified shocks, although the value of the maximum momentum is controlled, in our case, by a different mechanism. However, as in their case, the actual solution depends on the microphysics at the subshock, which determines the injection.

## 6. CONCLUSIONS

The assumption underlying most previous investigations of non-linear diffusive shock acceleration is the non-existence of waves able to scatter particles with energy above an upper cut-off. In this paper, we examine an alternative picture, in which the current generated by the

streaming cosmic rays falls below some critical value at a distance  $L_{\text{esc}}$  upstream of the subshock, and that beyond this the turbulence is insufficient to scatter the particles.

In terms of the non-linear response of the system to changes in the injection parameter, we find the two pictures are quite similar (see Fig. 1). One difference is that our spatial boundary method can be used to model the shape of the distribution close to the cut-off (see Fig. 3 and Fig. 4). This is an advantage because it potentially enables one to model the radiative signatures of the acceleration process.

The main difference, however, is that we are able to address the physics that determines the location of the boundary. Previous work that implemented such a boundary Vladimirov et al. (2006) did not constrain its location. In time-dependent models of acceleration in supernova remnants Berezhko & Völk (1997), an effective spatial boundary is imposed by the spherical geometry. But they assume a value for the amplified magnetic field in the entire computational box, without considering whether or not this is consistent with the location of the boundary.

We argue that the location of the boundary is determined by the growth rate of the instability responsible for field amplification. It has recently been shown that, in the case of efficient shock acceleration, a short-wavelength non-resonant mode Bell (2004) plays a crucial role. In a series of papers, Pelletier et al. (2006); Marcowith et al. (2006) argue that this non-resonant mode dominates far from the shock, while the resonant streaming instability takes over closer to the shock, driving the diffusion towards Bohm-type in the precu-

rior. According to these arguments, the position of the free-escape boundary should be fixed by the properties of the non-resonant mode, once the shock is modified by the cosmic-ray pressure. We show explicitly that the non-resonant modes are strongly driven at the escape boundary, and compare the local growth rate with the rate at which the waves are advected towards the shock front (see Fig. 6). In this picture, particles stream freely ahead (upstream) of the boundary, whereas behind (downstream of) it, the turbulence is assumed to be fully developed and particles undergo Bohm diffusion in an amplified magnetic field.

Zirakashvili & Ptuskin (2008) also suggest that the geometry of a supernova shock front sets the length scale for the precursor, and thus determines the maximum particle energy. However, we find that when the non-linear dynamics of the acceleration process are included, the length scale is set by the strength of the amplified magnetic field and the efficiency of the injection process. Ultimately, it is the microphysics of injection — represented in Figs. 1 and 6 by the parameter  $\nu$  — that determines not only the efficiency of the acceleration process, but also the maximum attainable particle energy.

This research was supported by a Grant from the G.I.F., the German-Israeli Foundation for Scientific Research and Development. PD thanks the MPI for Nuclear Physics for their hospitality during this work. BR gratefully acknowledges support from the Alexander von Humboldt foundation.

#### REFERENCES

- Achterberg, A. 1983, *A&A*, 119, 274  
 —. 1987, *A&A*, 174, 329  
 Amato, E., & Blasi, P. 2005, *MNRAS*, 364, L76  
 Amato, E., Blasi, P., & Gabici, S. 2008, *MNRAS*, 385, 1946  
 Bamba, A., Yamazaki, R., Yoshida, T., Terasawa, T., & Koyama, K. 2005, *ApJ*, 621, 793  
 Baring, M. G., & Kirk, J. G. 1991, *A&A*, 241, 329  
 Bell, A. R. 1978, *MNRAS*, 182, 147  
 —. 1987, *MNRAS*, 225, 615  
 —. 2004, *MNRAS*, 353, 550  
 —. 2005, *MNRAS*, 358, 181  
 Berezhko, E. G., & Völk, H. J. 1997, *Astroparticle Physics*, 7, 183  
 Blasi, P. 2002, *Astroparticle Physics*, 16, 429  
 Blasi, P., Amato, E., & Caprioli, D. 2007, *MNRAS*, 375, 1471  
 Bykov, A. M., & Toptygin, I. N. 2005, *Astronomy Letters*, 31, 748  
 Caprioli, D., Blasi, P., Amato, E. & Vietri, M. 2008, *ApJ*, 679, 139  
 Drury, L. O., & Voelk, J. H. 1981, *ApJ*, 248, 344  
 Falle, S. A. E. G., & Giddings, J. R. 1987, *MNRAS*, 225, 399  
 Hwang, U., Decourchelle, A., Holt, S. S., & Petre, R. 2002, *ApJ*, 581, 1101  
 Kirk, J. G. 1990, *A&A*, 239, 404  
 Landau, L. D., & Lifshitz, E. M. 1959, *Fluid mechanics (Course of theoretical physics, Oxford: Pergamon Press, 1959)*  
 Lucek, S. G., & Bell, A. R. 2000, *MNRAS*, 314, 65  
 MacKenzie, J. F., & Voelk, H. J. 1982, *A&A*, 116, 191  
 Malkov, M. A. 1997a, *ApJ*, 485, 638  
 —. 1997b, *ApJ*, 491, 584  
 Malkov, M. A., Diamond, P. H., & Völk, H. J. 2000, *ApJ*, 533, L171  
 Malkov, M. A., & Drury, L. O. 2001, *Reports of Progress in Physics*, 64, 429  
 Marcowith, A., Lemoine, M., & Pelletier, G. 2006, *A&A*, 453, 193  
 Niemiec, J., Pohl, M., Stroman, T., & Nishikawa, K.-I. 2008, *ApJ*, 684, 1174  
 Pelletier, G., Lemoine, M., & Marcowith, A. 2006, *A&A*, 453, 181  
 Reville, B., Kirk, J. G., Duffy, P., & O’Sullivan, S. 2007, *A&A*, 475, 435  
 Reville, B., O’Sullivan, S., Duffy, P., & Kirk, J. G. 2008, *MNRAS*, 386, 509  
 Riquelme, M. A. and Spitkovsky, A. 2008, *ApJ* submitted; arXiv:0810.4565  
 Skilling, J. 1975, *MNRAS*, 172, 557  
 Uchiyama, Y., Aharonian, F. A., Tanaka, T., Takahashi, T., & Maeda, Y. 2007, *Nature*, 449, 576  
 Vink, J., & Laming, J. M. 2003, *ApJ*, 584, 758  
 Vladimirov, A., Ellison, D. C., & Bykov, A. 2006, *ApJ*, 652, 1246  
 Vladimirov, A., Bykov, A., & Ellison, D., 2008, *ApJ*, 688, 1084  
 Zank, G. P., Webb, G. M., & Donohue, D. J. 1993, *ApJ*, 406, 67  
 Zirakashvili, V. N., & Ptuskin, V. S. 2008, *ApJ*, 678, 939  
 Zirakashvili, V. N., Ptuskin, V. S., & Völk, H. J. 2008, *ApJ*, 678, 255